Interactions of Precipitation/Dissolution Waves and Ion Exchange in Flow Through Permeable Media

This paper describes reactive flow in permeable media based on a numerical model that assumes local thermodynamic equilibrium. The model simulates single-phase, one-dimensional flow with greater generality than any model in the current literature. The mathematical foundation for the formulation is discussed in some detail. Results for hypothetical examples demonstrate that ion exchange and precipitation/dissolution of solids can interact to produce wave behavior not possible with either phenomenon alone. An important application involving both ion exchange and precipitation/dissolution is alkaline flooding. Model predictions for several laboratory alkaline floods indicate that the assumption of equilibrium is justified for these experiments. Simple calculations based on the equilibrium theory provide estimates of pH loss and hydroxide penetration distance.

S. L. Bryant, R. S. Schechter and L. W. Lake
Department of Petroleum Engineering
The University of Texas
Austin, TX 78712

SCOPE

Flow of fluid through a permeable medium is accompanied by a variety of effects that form the basis for many scientific, industrial, and engineering processes. Such flow can displace fluids originally contained in the medium, as in secondary oil recovery (Collins, 1961), and can also induce changes in the injected fluid, as in numerous sorption processes (Treybal, 1968) or heterogeneous catalysis (Levenspiel, 1962). The flow may even change the medium itself, as in ore leaching (Kabir et al., 1982) or permeability treatments (Walsh et al., 1983). Because of this diversity a general model of flow in permeable media would be widely applicable.

A mechanism important in reactive flows is ion exchange. Numerous separation processes, such as water desalination, radioisotope isolation, and production of antibiotics, are based on ion exchange, and the theory of exchange is well established (Vermeulen et al., 1973; Treybal, 1968).

Another important mechanism in reactive flow is precipitation and dissolution. A wide variety of natural flows are affected by the formation and transport of solids, including alkaline flooding (De Zabala et al., 1982), steam flooding (Reed, 1980), sandstone acidizing (Shaughnessy and Kunze, 1981; Walsh et al., 1982), near wellbore scaling (Vetter and Kandarpa, 1980), and mineral leaching (Tatom et al., 1981; Gao et al., 1981). Unlike ion exchange, the equilibrium relations for precipitation/dissolution do not provide a definite relation between fluid and solid phase concentrations. Nevertheless, propagation of precipitation/dissolution waves occurs in a chromatographic manner, and their strength and velocity can be calculated from the coherence and the "downstream equilibrium" conditions (Walsh et al., 1984).

Previous investigations have considered ion exchange (Helfferich and Klein, 1970) and precipitation/dissolution individually (Walsh et al., 1984); however, both phenomena occur in many applications. This paper presents a model that accounts for ion exchange, precipitation and dissolution of minerals, adsorption, formation of ion complexes in solution, electron transfer, and nonideal solutions (Walsh, 1983). The model

assumes local thermodynamic equilibrium. Using this general flow model, we present a hypothetical example that examines the interactions between exchange waves and precipitation/dissolution waves. We then apply the model to alkaline flooding.

CONCLUSIONS AND SIGNIFICANCE

Our equilibrium flow model simulates single-phase reactive flow in permeable media in great generality. Even when nonequilibrium effects are significant, a qualitative description of wave behavior can be obtained; quantitative predictions are possible in many cases.

The model indicates that ion exchange waves and precipitation/dissolution waves can interact to produce complex behavior. Such behavior is the rule rather than the exception, but it cannot occur if exchange and precipitation/dissolution are considered separately. For example, precipitation waves, which are sharp when only precipitation/dissolution reactions are possible, can become spreading waves when a component of the precipitate is also involved in an exchange reaction. Conversely, a dissolution wave can interject a constant-state region into a spreading exchange wave. Hence, accurate simulation of flows in which exchange and precipitation/dissolution are important must account for both phenomena.

Simulations of laboratory alkaline floods match reported effluent analyses, indicating that the assumption of local equilibrium accurately describes many floods. In these simulations a representative set of minerals was chosen to demonstrate possible behavior. The model confirms the importance of clay mineral reactions.

The local equilibrium assumption leads to a simple method of evaluating alkaline floods. The pH loss can be attributed primarily to silica dissolution, and hydroxide penetration distance depends primarily on exchange reactions involving the hydroxide counterion. These observations suggest simple procedures for estimating pH loss and hydroxide penetration.

Mathematical Development

Modeling fluid flow in permeable media

Many physical and chemical factors influence flow in permeable media. Altering the fluid content of a medium by displacement depends primarily on physical parameters such as fluid densities and viscosities, relative permeabilities, and heterogeneity of the medium. On the other hand, altering the composition of the flowing fluid or the medium itself depends primarily on chemical interactions such as adsorption or mineral dissolution. Thus a completely general model of flow in permeable media must account for both the chemistry and the physics of the problem, a computationally expensive undertaking.

Fortunately many practical problems permit some simplifying assumptions. For many single-phase flow applications the chief interest lies in compositional changes caused by the flow. In this paper we present a single-phase flow model that allows for precipitation and dissolution of minerals, adsorption, ion exchange, oxidation-reduction reactions, activity coefficient corrections, and formation of ion complexes.

The model makes several assumptions:

1. The medium is one-dimensional, homogeneous and of constant porosity.
2. Changes in density and viscosity with composition and pressure are small.
3. Supersaturation in the flowing phase is not permitted.
4. The flow is isothermal.
5. Solid phases are stationary so precipitates cannot migrate by entrainment in the flowing phase.

The last assumption does not prohibit the advance of solids or sorbed species through the medium, since a solid may precipitate anywhere its solubility product is exceeded.

The primary assumption concerning the chemistry is that thermodynamic equilibrium is attained at every point of the medium. Most fluid-phase reactions are fast enough to justify this assumption for the flowing phase, and the low velocity of natural flows allows many reactions between the flowing and stationary phases to approach equilibrium.

Subject to these assumptions, the transport of species through the medium is described by a set of partial differential equations describing the conservation of mass:

$$\partial(\phi C_i^T)/\partial t + u\,\partial\{h_{ij}C_j\}/\partial x - \partial^2\{\phi K_{\ell j} h_{ij} C_j\}/\partial x^2 = 0, \qquad i = 1, \ldots, I \quad (1)$$

where I is the number of chemical elements in the system, $C_i^T(x, t)$ is the total concentration of element i, C_j is the concentration of species j ($j = 1 \ldots J$) in the flowing phase, and h_{ij} is the stoichiometric coefficient of element i in the species j. The remaining terms are defined in the Notation. In this and all subsequent equations (unless noted) a repeated subscript in multiplied terms means a sum over the entire subscript range. Hence, the expression $h_{ij}C_j$ is equivalent to $\Sigma_{j=1}^{J} h_{ij}C_j$. Contributions from the stationary phases as well as the flowing phase are included in the total concentration, C_i^T, given by

$$C_i^T = h_{ij}C_j + g_{ik}\hat{C}_k + f_{i\ell}\overline{C}_\ell \quad i = 1, \ldots, I \qquad (2)$$

where $\hat{C}_k(x, t)$ is the concentration of mineral k ($k = 1 \ldots K$) and $\overline{C}_\ell(x, t)$ is the concentration of bound species ℓ ($\ell = 1 \ldots L$). Note that Eq. 1 contains no spatial derivatives of stationary phase concentrations, $\hat{C}_k$ and $\overline{C}_\ell$, because there is no flux of the solid phases.

We cast Eq. 1 in dimensionless form by introducing dimensionless variables

$$x_D = x/L; \quad t_D = ut/\phi L; \quad N_{Pe} = uL/K_\ell\phi \tag{3}$$

yielding

$$\partial C_i^T/\partial t_D + \partial\{h_{ij}C_j\}/\partial x_D - (N_{Pe})^{-1}\partial^2\{h_{ij}C_j\}/\partial x_D^2 = 0, \quad i = 1, \ldots, I \tag{4}$$

for $C_i^T(x_D,t_D)$. In writing Eq. 4 we have assumed that the dispersion coefficients $K_{\ell j}$ are equal for all species j.

To determine the particular solution to the set of differential equations, Eq. 4, boundary conditions must be provided. We anticipate a finite-difference solution in which numerical dispersion approximates physical dispersion, thereby reducing the order of the equations to be solved. Thus it suffices to provide the initial conditions $[C_i^T(x_D,0), i = 1, \ldots, I]$ and the injected conditions $[C_i^T(0,t_D), i = 1, \ldots, I]$. The actual compositions corresponding to these totals are determined by the equilibrium relations (Lake et al., 1984). The injected composition must not include solids, of course, since there is no flux of the solid phases.

We consider only a uniform initial state and a constant injected composition. A problem satisfying these conditions is a member of the class of Riemann problems. A useful feature of Riemann problems is that their solutions are self-similar. For one-dimensional nondispersive flow, self-similarity means that the solution can be described in terms of the single parameter x_D/t_D (Rhee et al., 1968; Lax, 1957). This property makes wave theory a convenient means of describing the problem solution, even though the solution technique is numerical.

Formulation of the model

The flow model discussed in this paper is an extension of a model first presented by Walsh (1983). In its original form, the model allowed for mineral precipitation/dissolution, formation of ion complexes in solution, oxidation-reduction reactions, and activity corrections. It successfully simulated well stimulation by acid (Walsh et al., 1982), transport of gelling agents (Walsh et al., 1983), and geological deposition and leaching of uranium ore (Walsh et al., 1984). To extend the application of the model we have incorporated ion exchange (sorption of aqueous species) into the formulation, making it the most general simulator of its kind reported in the literature (Miller and Benson, 1983). In this section we elaborate upon the mathematical foundation for the model. For the sake of brevity we will not discuss redox reactions or activity corrections in this paper. The treatment of these (Walsh, 1983) is easily generalized to this discussion.

A set of I partial differential equations describes the transport of species through the medium. Solution of this set of equations is obtained numerically by an explicit, backward-in-space finite-difference scheme. The scheme is equivalent to a series of batch equilibrium calculations. During one time step the fluid in a grid block flows into the next grid block downstream. Since the scheme is backward in space, the composition of the fluid entering the grid block is known; since the scheme is explicit, the composition of the (stationary) solid phase remaining in the grid block is also known. Hence the total elemental concentrations in the grid block after one time step are determined. We may therefore calculate the new equilibrium state of the grid block with the following procedure, Figure 1.

We consider a system of $j = 1, \ldots, J$ fluid phase species and $k = 1, \ldots, K$ possible solids, consisting of $i = 1, \ldots, I$ different elements. From the set of J species we may select a subset of I independent species to form the basis for writing chemical reactions. The species in this subset are independent in the sense that

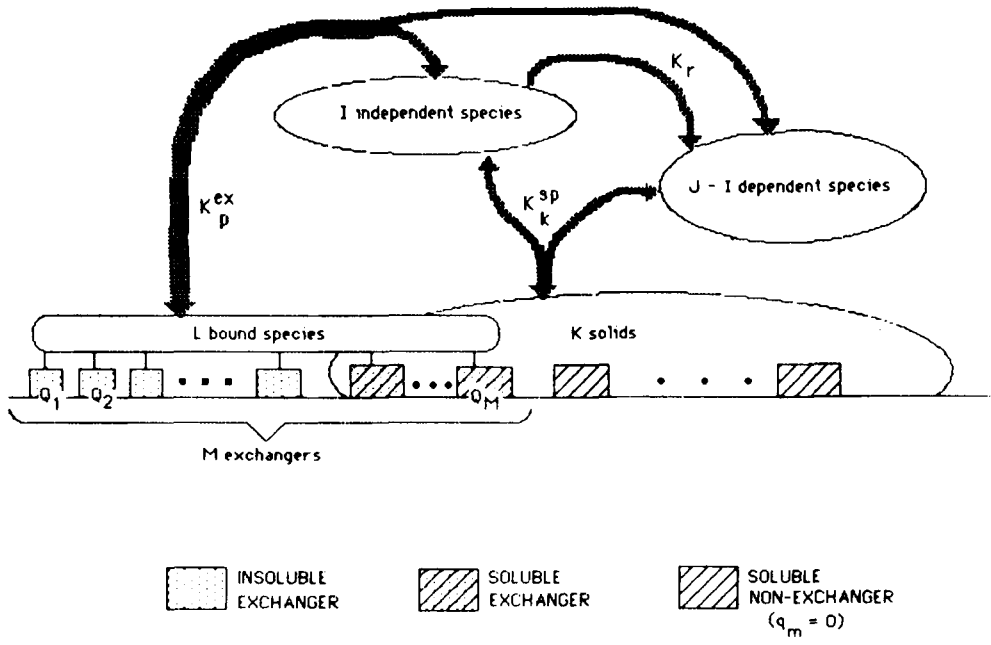

Figure 1. Schematic diagram for equilibrium calculation.

the formula vector of any species (i.e., the vector of subscripts in the molecular formula for that species) in the subset is not a linear combination of the formula vectors for the other species in the subset (Smith and Missen, 1982). This independence insures the determinacy of the system of equations that follow.

There are $J - I$ equilibrium expressions of the form

$$K_r = C_j^{\nu_{rj}} \quad r = I + 1, \ldots, J \tag{5}$$

that relate the concentrations of the dependent species (the ones not included in the basis set of I species) to the independent species. In writing Eq. 5 we adopt the convention that multiplication occurs over repeated indices in the subscripts of bases and exponents. Hence, the righthand side of Eq. 5 is equivalent to $\Pi_{j=1}^{J} C_j^{\nu_{rj}}$. The set of Eq. 5 can be rewritten so that only one dependent species appears in each equation. Each dependent species concentration can then be expressed in terms of the independent species concentrations only. We denote the concentration of dependent species r by P_r, $r = I + 1, \ldots, J$. A charge balance for the fluid phase may be imposed upon the concentrations C_j, as discussed in the appendix.

There are K solubility product constraints, one for each possible mineral, of the form

$$K_k^{sp} \geq C_j^{w_{kj}} \quad k = 1, \ldots, K \tag{6}$$

The constraint for mineral k becomes an equality when that mineral is present. Thus introduction of an unknown mineral concentration is always accompanied by the addition of a solubility product equation. The number of solids present must be less than the number of elements, $K \leq I$, otherwise Eqs. 5 and 6 will overconstrain the fluid-phase compositions.

Any of the J species in the fluid phase may exchange on one or several substrates; a species j that exchanges on $m_j = 1 \ldots M$ substrates counts as m_j distinct bound species. Hence the number of bound species L may be greater than J. Any of the K solids may act as a substrate. We assign a specific exchange capacity (or specific adsorption site concentration) q_m to each of the K solids, assuming that solid surface area is proportional to solid mass. The exchange/adsorption capacity per unit pore volume, Q_m, of solid m is then given by

$$Q_m = q_m \hat{C}_m \quad \text{(no sum)} \quad m = 1, \ldots, M \tag{7}$$

A solid that does not sorb species is given $q_m = 0$.

We allow an additional set of solids that sorb species but do not dissolve or precipitate. These insoluble substrates necessarily have constant concentrations and exchange/adsorption capacities. Since the solution procedure need not distinguish between soluble and insoluble substrates once the exchange/adsorption capacities are determined, the exchange/adsorption capacities of the insoluble substrates are also denoted by Q_m. The inclusion of insoluble substrates means that the total number of substrates M may exceed the total number of soluble solids, K.

There are M surface site balances, one for each substrate, of the form

$$Q_m = z_{m\ell} \bar{C}_\ell \quad m = 1, \ldots, M \tag{8}$$

where $z_{m\ell}$ measures the number of sites occupied by sorbed species ℓ on substrate m. If a species ℓ does not sorb on substrate m, its contribution $z_{m\ell}$ is zero. Vacant sites on a substrate may be accounted for by including a concentration $\bar{C}_v$, with $z_{mv} = 1$, among the $\bar{C}_\ell$.

For a given number of sorbed species there are one fewer exchange/adsorption equilibria relations. Therefore we must have a total of $L - M$ exchange/adsorption equilibria, of the form

$$K_p^{ex} = (C_j^{y_{pj}})(\bar{C}_\ell^{x_{p\ell}}) \quad p = 1, \ldots, L - M \tag{9}$$

Equation 9 reduces to a Langmuir-type adsorption isotherm when a concentration of vacant sites $\bar{C}_v$ is included. For example, let species 1 adsorb on substrate 1 according to

$$K_1 = \bar{C}_1/(C_1 \bar{C}_v) \tag{9a}$$

Using the appropriate site balance, Eq. 8, to eliminate $\bar{C}_v$ and rearranging, we obtain

$$\bar{C}_1 = \frac{K_1 C_1 Q_1}{1 + K_1 C_1} \tag{9b}$$

where we assume $z_{11} = 1$. Analogous expressions for competitive adsorption are readily obtained. This model of exchange/adsorption processes, Eqs. 7–9, does not consider the detailed physics of such processes (Lyklema, 1984), but it does provide a general working tool.

There are a total of $I + J + K + L$ unknowns (C_i^T for $i = 1, \ldots, I$; C_j for $j = 1, \ldots, J$; $\hat{C}_k$ for $k = 1, \ldots, K$; and $\bar{C}_\ell$ for $\ell = 1, \ldots, L$); and a like number of equations (Eqs. 2, 4, 5, 6, 8, and 9), so that the system is determined.

Since we cannot know a priori which solids will be present at equilibrium, the grid block equilibrium calculation is iterative. We initiate the process by assuming that the solids present at the previous time step will also exist in the new equilibrium state. The new concentrations of these solids, the flowing phase species and the bound species, are then calculated, and the solubility product constraints of all possible solids are checked. If any constraints are exceeded, the corresponding solids are added in the order in which they exceed the solubility product. The concentrations are then recalculated. When all constraints are satisfied with no negative concentrations, the correct assemblage of solids has been found. Note that since we allow all solids to be exchangers, the number of sorbing species may vary from iteration to iteration, depending on which solids are present. An outline of one iteration of this procedure is given in the appendix.

Exchange Waves, Precipitation/Dissolution Waves and Their Interactions

Representing Waves

Injecting a fluid of composition different from the initial fluid will perturb a system. The system responds to this perturbation by forming a series of concentration changes or waves propagating through the medium. Viewed from a stationary point in the medium, this wave series comprises a path through composition space, each point of which represents a state of equilibrium between fluid and medium. As injection continues, the medium ultimately reaches an "injected" state in which the entire medium has equilibrated with the injected fluid, and further injection produces no changes in composition. The series of waves thus connects the initial state to the injected state by a

sequence of transitions between intermediate equilibrium states. A single inlet perturbation may give rise to several waves.

The first (fastest moving) wave in a series marks the displacement of the fluid initially present in the medium, and thus it moves with the velocity of the injected fluid u/ϕ. Species that undergo no chemical interactions with the medium (chloride is a common example) pass unhindered through the medium. The unretarded fluid-phase concentration change is often called the salinity wave.

Chemical interactions between flowing and stationary phases produce more complex behavior. If a reactive fluid is injected into a medium, noninteracting species still move in the salinity wave. However, the advance of reactive species is retarded, resulting in a series of successively slower waves moving behind the salinity wave. The final (i.e., slowest moving) wave marks the advance of injected fluid unaltered in composition. Compositions between waves may differ radically from the initial and injected compositions.

The most convenient way to display waves is the time-distance diagram, wherein dimensionless distance, x_D, is plotted vs. dimensionless time, t_D. Curves of constant composition on these coordinates indicate the propagation of waves. The time axis ($x_D = 0$) represents the injected conditions; the distance axis ($t_D = 0$) the initial conditions. The initial and injected compositions both exist at the origin ($x_D = t_D = 0$), which represents the inlet perturbation. The waves resulting from this perturbation are thus represented by a series of curves emanating from the origin. Since the solution to a Riemann problem can be expressed in terms of the ratio x_D/t_D, these curves will be straight lines.

A shock wave is a sharp transition from one concentration plateau to another, and it is represented as a single line on the diagram. The area immediately above the line is the region of constant concentration ahead of the shock wave; the area immediately below is the region of constant concentration behind the shock. A spreading wave is a gradual transition between plateaus; the leading edge of the wave moves faster than the trailing edge, resulting in a region of smoothly varying concentrations between the edges. Thus a spreading wave on an x_D–t_D diagram is a bundle of lines between two bounding lines that indicate the leading and trailing edges of the wave. The bundle of lines are replaced by shaded areas in the accompanying diagrams. The slope of a line on a diagram indicates the velocity of the corresponding concentration as a fraction of the velocity of the injected fluid (specific velocity). Hence the salinity wave (in the absence of dispersion) will be represented as a unit slope line. Subsequent waves will be represented as lines with successively smaller slopes.

Equilibrium Relations for Ion Exchange and Precipitation/Dissolution

Precipitation/dissolution and ion exchange waves result from chemical interaction between flowing phase and stationary phase(s). However, the nature of the interaction for each is different.

In ion exchange the concentrations in the stationary phase are continuous functions of concentrations in the flowing phase. Specification of the composition of one phase determines the composition of the other. A plot of bound species concentration, $\bar{C}_1$ in Figure 2a, against flowing phase concentration C_1, a sorption isotherm, is a smooth curve. The functions describing such isotherms are usually continuously differentiable, a property

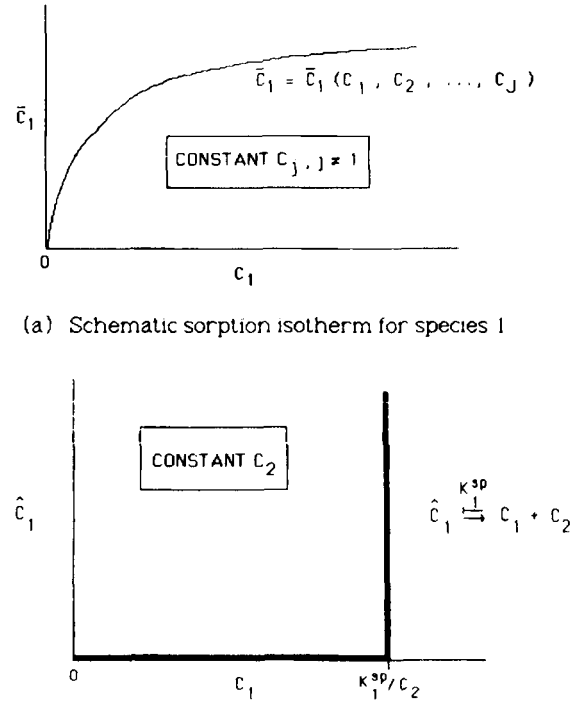

Figure 2. Equilibrium relations for ion exchange and precipitation/dissolution.

that gives rise to the notion of concentration velocities. The relative velocities of the concentrations within a wave determine the spreading or sharpening nature of that wave (Helfferich and Klein, 1970). Hence, exchange waves may sharpen or spread as they propagate. The series of waves in a typical exchange problem consists of a salinity wave followed by an exchange wave that marks the transition of the exchanger from its initial state to a state in equilibrium with the injected fluid.

In precipitation/dissolution problems there is no continuous function relating concentrations in the flowing phase to concentrations in the solid phase, and specification of the composition of one phase does not determine the composition of the other. This is because the solubility product constraints defining precipitation/dissolution are inequalities (e.g., Eq. 6) that become equalities only when the corresponding solid is present. Note that a solubility product constraint does not involve the concentration of the solid. Thus a precipitation isotherm, defined as the concentration of the solid, $\hat{C}_1$, in Figure 2b, plotted against the flowing phase concentration C_1 of a component of the solid, would have a discontinuous first derivative. Clearly, the notion of concentration velocity defined for sorption isotherms cannot be rigorously applied to such precipitation isotherms. Nonetheless, Bryant (1985) shows that precipitation/dissolution waves are quite sharp; even in the presence of dispersion they may be assumed shocks. A typical precipitation/dissolution problem thus consists of a salinity wave followed by shocks marking transitions between regions of constant concentrations. Each region contains a different suite of minerals. In the final region the medium reaches the injected state, wherein all initially present minerals that are soluble in the injected fluid are completely dissolved.

Table 1. Data for Sodium/Calcium Exchange, Fig. 3

Species	Concentration kmol/m³ of Pore Volume Init.	Inj.
Na^+	0.0297	0.0497
Ca^{++}	0.00515	0.00515
Cl^-	0.0400	0.0600
Na(sorbed)	0.0044	(0.007)
Ca(sorbed)	0.0155	(0.0142)

Exchange parameters:

$$(C_{Na^+}/\bar{C}_{Na})^2/(C_{Ca^{++}}/\bar{C}_{Ca}) = 139$$

$$\bar{C}_{Na} + 2\bar{C}_{Ca} = 0.0354 = Q_1$$

Dispersion Coefficient:

$$N_{Pe}^{-1} = 0.001$$

Predicted Wave Behavior

To confirm the correctness of the model, we simulated a core flood reported in Lake and Helfferich (1978). Sodium-calcium exchange was the only important fluid-solid interaction, and there was only one insoluble exchanger. Data for the simulation are given in Table 1. (In this and all subsequent tables, the sorbed concentrations listed in parentheses for the injected fluids are those that will prevail after the slowest wave. As mentioned above, solid species do not flow.) The fluid injected into the core contained a higher sodium concentration than the fluid initially present. To equilibrate with the higher sodium concentration, the medium must replace some sorbed calcium ions with sodium ions. Since clays typically prefer the doubly charged calcium ion to the singly charged sodium ion, this displacement is not efficient, and a spreading exchange wave results. Predicted effluent calcium concentrations agree with observed data, shown in Figure 3a.

A time-distance representation of the simulation is shown in Figure 3b. The salinity wave *Sa* and spreading exchange wave *Ex* appear as envelopes of smoothly varying concentrations between the initial conditions *I* and injected conditions *II*. Dispersion in the finite-difference solution and in the experiment blurs the boundaries of both waves, so that the constant state that theoretically exists between *Sa* and *Ex* is not present. The theoretical solution may be inferred from the finite-difference solution; the time-distance diagrams for subsequent examples depict the inferred theoretical solution.

When ion exchange and precipitation/dissolution interact, one might expect the two types of waves to separate the medium into a precipitation/dissolution regime and an exchange regime. If so, one could then treat the problem by superimposing the individual behaviors. Rather than separating, however, precipitation/dissolution waves can merge with exchange waves, altering the characteristics of both in ways not possible with either phenomenon alone.

Figure 4 schematically depicts several hypothetical examples of precipitation/dissolution-exchange interactions:

1. Exchange (*C* and *D* on *AB*) on a soluble substrate (*AB*).
2. Exchange (*C* and *A*) on an insoluble substrate and a soluble solid (*AB*) initially present which contains an exchanging species (*A*).
3. Exchange (*C* and *D*) on an insoluble substrate and a solubility product constraint on an exchanging species (*D*).

These examples hardly constitute a catalog of all possible behav-

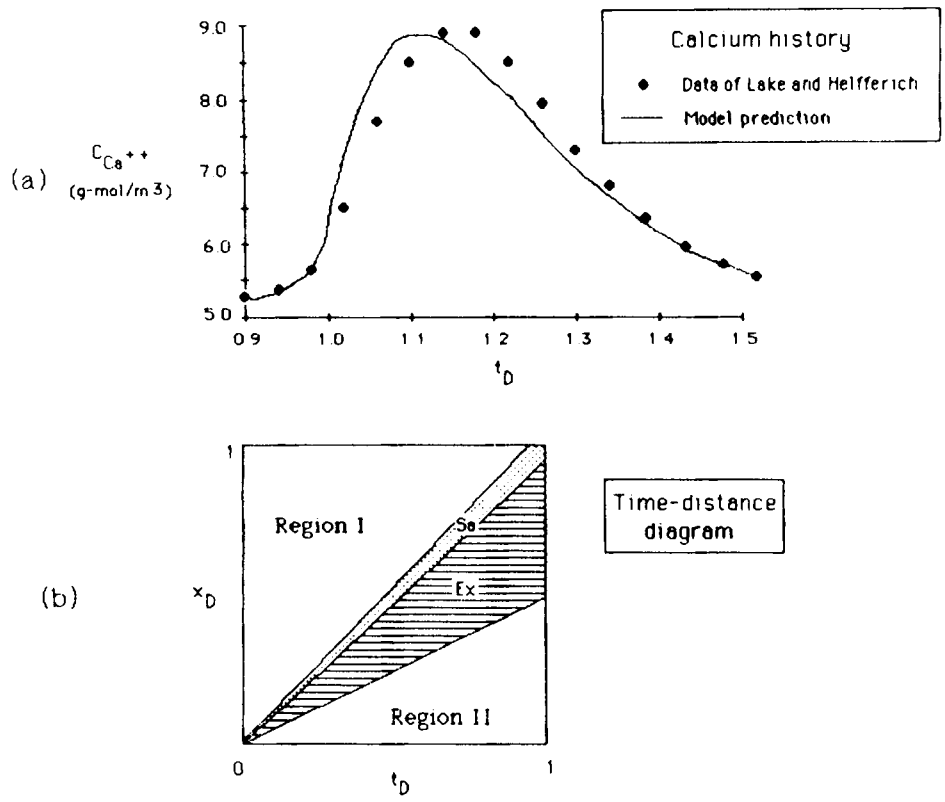

Figure 3. Model predictions for sodium-calcium exchange problem.

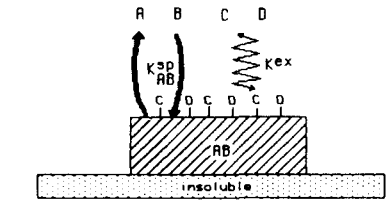

(a) C and D exchange on soluble substrate AB

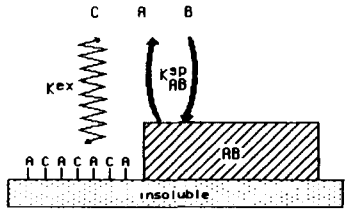

(b) A and C exchange on an insoluble substrate; solid AB is initially present

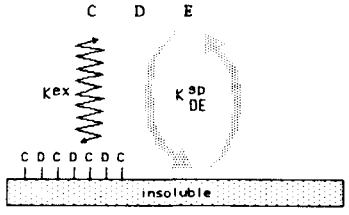

(c) C and D exchange on an insoluble substrate, D and E can precipitate solid DE

Figure 4. Schematic diagram of interactions between ion exchange and precipitation/dissolution of solids.

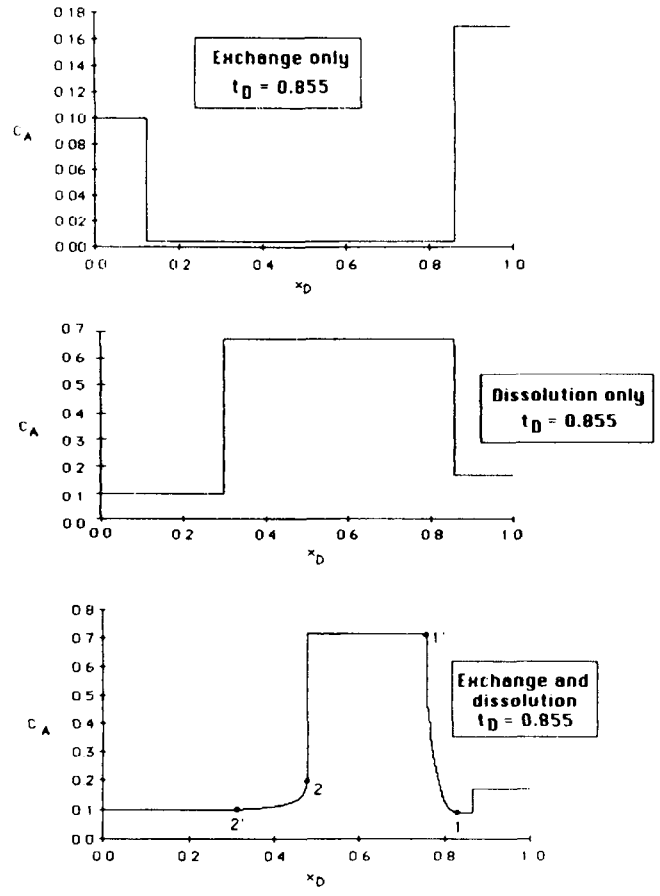

Figure 5. Profiles for exchange in the presence of a solid containing an exchanging species.

ior, but we can illustrate the point that ion exchange and precipitation/dissolution waves do not superpose with one example.

Figure 4b shows an example in which aqueous species A and C exchange on an insoluble substrate while solid AB may dissolve according to

$$AB(s) = A + B, \quad K^{SP}_{AB} = C_A C_B \tag{10}$$

There are now two sources for A: from dissolution of AB and from exchange on the insoluble substrate. Table 2 shows the initial and injected compositions and the solubility and isotherm constants. Solid AB is not an exchanger. The results of the displacement are shown in Figure 5 as profiles at $t_D = 0.855$, and in Figure 6 as time-distance diagrams.

Table 2. Data for Sharp Exchange on Insoluble Substrate with Solid Containing Exchanging Species Initially Present

	Concentration (Arbitrary Units)					
	Figure 6a		Figure 6b		Figure 6c	
Species	Init.	Inj.	Init.	Inj.	Init.	Inj.
A	0.169	0.10	0.169	0.10	0.169	0.10
B	2.50	0.05	2.50	0.05	2.50	0.05
C	8.538	0.10	8.538	0.10	8.538	0.10
AB(s)	0.0	0	1.0	0	1.0	0
A(sorbed)	0.131	(0.722)	—	—	0.131	(0.722)
C(sorbed)	0.663	(0.072)	—	—	0.633	(0.072)

$K^{sp}_{AB} = 0.427$

Exchange parameters: $\overline{C}_A + \overline{C}_C = 0.794$
$C_A/C_C * \overline{C}_C/\overline{C}_A = 0.1$

If solid AB is not present (upper panel in Figures 5 and 6), ion exchange causes a pistonlike displacement of the C originally bound to the clays. The drop in C_A between $x_D = 0.855$ and 0.12 is caused by the A being depleted from solution to satisfy the exchange sites vacated by C.

When the exchange capacity is set to zero (middle panel in Figures 5 and 6), there is a plateau in C_A between $x_D = 0.855$ and 0.33 that is greater than the concentrations of A injected or initially present. (Note the change of scales on the plots of Figure 5.) This A is from the dissolution of AB occurring at the dissolution wave, which is, of course, a shock.

When exchange and dissolution are both present (bottom panel in Figures 5 and 6) the character of the displacement changes drastically. Exchange now takes place over two waves, 1 to 1′ and 2 to 2′, and neither wave is a shock. The dissolution wave remains a shock, however. This is not a general result, though, because we have observed cases in which precipitation/dissolution waves are spreading (Bryant, 1985).

The concentration profile in the bottom panel of Figure 5 has the following interpretation. The ion exchange reaction causes C_A to fall at $x_D = 0.855$ as in the exchange-only case. This plateau is shortly interrupted by the products of the dissolution reaction that increase C_A. The increased A concentration loads the insoluble exchanger, which subsequently attains its injected state across the exchange wave from 2 to 2′.

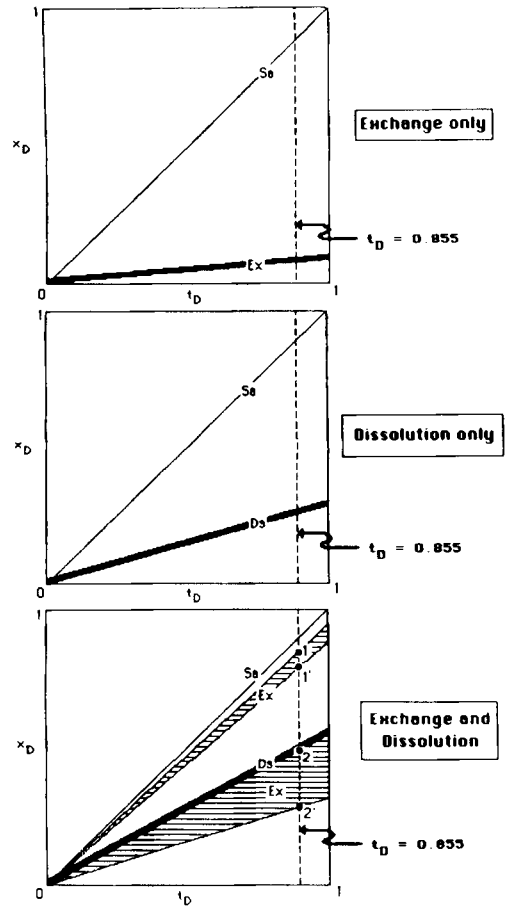

Figure 6. Time-distance diagrams for example of Fig. 5.

More complicated cases are easily constructed (Bryant, 1985). This single case illustrates that ignoring either mechanism can lead to an incorrect interpretation of the wave response, and that the two phenomena do not superimpose as would be suggested by the time-distance diagrams in the upper two panels of Figure 6.

A Practical Example

While the interaction of exchange and precipitation/dissolution is of considerable theoretical interest, there also exist practical cases in which these interactions are important. If we inject a pH 9 solution of Na_2CO_3 into a reservoir in which the clays are in the calcium state, for example, the calcium ions displaced from the clays may precipitate the carbonate ions to form calcite, $CaCO_3$. For realistic exchange parameters and solubility constraint, Table 3, the model predicts significant calcite precipitation, shown in Figure 7. The fluid phase calcium concentrations in the plateau behind the exchange wave are almost as low as the injected concentration. The elution of this plateau in a core flood makes it appear that most of the calcium has been removed from the core, when in fact a significant concentration of calcite remains.

Problems such as these cannot be simulated by considering exchange and precipitation/dissolution separately, since vital features of the wave response may depend on interactions of the phenomena.

Table 3. Data for Na_2CO_3 Flood of a Calcium-Containing Rock, Fig. 7

Species	Concentration kmol/m³ of Pore Volume Init.	Inj.
Na^+	0.068	0.015
Ca^{++}	0.015	0.000001
$CO_3^=$	0.0000002	0.0049
HCO_3^-	0.0000008	0.0051
Cl^-	0.096	0.0
OH^-	0.000019	0.000077
Ca(sorbed)	0.035	(0.0026)
Na(sorbed)	0.029	(0.0948)

$K_{CaCO_3} = (C_{Ca^{++}})(C_{CO_3^=}) = 6.3 \times 10^{-9}$ (kmol/m³ · PV)²

Exchange parameters: $(C_{Na^+}/\bar{C}_{Na})^2/(C_{Ca^{++}}/\bar{C}_{Ca}) = 12.2$

$\bar{C}_{Na} + 2\bar{C}_{Ca} = 0.10$ kmol sorbed/m³ · PV

Implications for Alkaline Flooding

Modeling Alkaline Floods

An important application involving both precipitation/dissolution and cation exchange is oil recovery by injection of high-pH solutions. The alkaline solution neutralizes organic acids in the oil, thereby mobilizing the oil by a variety of mechanisms (De Zabala et al., 1982). For a flood to be successful, the alkaline agent must not be depleted below some threshold pH (Cooke et al., 1974); for a flood to be economic, the alkaline agent must penetrate as far as possible into the reservoir. The amount of depletion and the degree of penetration depend primarily on interaction of the alkaline agent with the reservoir rock.

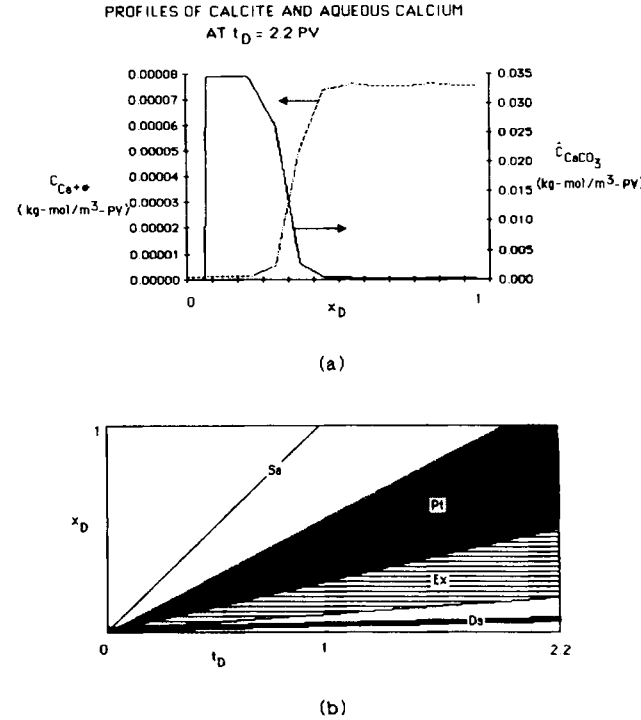

Figure 7. Simulation of Na_2CO_3 injection into calcium-loaded rock.

The reaction responsible for most of the hydroxide consumption is the dissolution of quartz (Bunge and Radke, 1982; Southwick, 1984; Sydansk, 1982; Mohnot et al., 1984). Reactions involving clay minerals may also consume hydroxide (Mohnot et al., 1984; Boon et al., 1983; Surdam and Sheppard, 1978; Garrels and Christ, 1965; Drever, 1982; Sydansk, 1982) and affect permeability (Boon et al., 1983). The pH drops from its injected value due to these reactions, and we refer to this drop as the pH loss.

Exchange between the alkali counterion (usually sodium) and ions already held by the rock strongly influences the speed of propagation of alkaline agent. As pointed out in the example above, both precipitation/dissolution and ion exchange must be taken into account for correct simulation of wave behavior. Our equilibrium model could produce a detailed study of the alkaline flooding, but the lack of experimental detail and thermodynamic data do not warrant it. Thus we will make some simplifying assumptions about the process.

First, we shall use a generic reservoir mineralogy. This is a reasonable approximation since alkaline flooding is most often done in sandstones, which are mostly quartz. A wide variety of highly reactive minerals and clays make up the small nonquartz fraction of a typical sandstone in concentrations that can vary greatly in different sandstones (Crocker et al., 1983). Instead of including all possible clays, for which reliable solubility product data are scarce, we use kaolinite and muscovite to represent two-layer and three-layer clays initially present in the sandstone, and analcite to represent clays stable in high-pH, high-salinity solutions.

Second, we do not explicitly account for the presence of the oil phase. We are primarily concerned with the transport of the alkaline agent, which is influenced chiefly by chemical interactions. Bunge and Radke (1982) note that hydroxide breakthrough times for several floods in oil-containing sandstone cores can be predicted by (single-phase) chromatography theory. Thus, the presence of oil does not seem to prevent the alkaline agent from contacting the reservoir rock.

Finally, although the low velocities in field applications should permit even rather slow reactions to approach equilibrium, there is controversy about how to model some reactions, especially the dissolution of silica. Southwick (1984) and others (Mohnot et al., 1984) argue that silica dissolution proceeds to equilibrium in field time scales. However, others (Sydansk, 1982; Bunge and Radke, 1982) present core flood data that demonstrate a kinetic limitation on silica dissolution. Even if local thermodynamic equilibrium is not a good approximation, our assumption of equilibrium yields conservative estimates of alkaline flood behavior because maximum pH loss occurs when hydroxide-consuming reactions proceed to equilibrium. Penetration of alkaline agent also depends on losses suffered. The model will generally overestimate pH losses and underestimate penetration distance for a flood that is subject to kinetic or mass-transfer limitations.

Comparison with Experimental Data

Bunge and Radke (1982) report the effluent history of a typical alkaline flood in an oil-bearing core, with delayed hydroxide breakthrough and subsequent plateaus in effluent Si and Al concentrations. The concentration plateaus suggest that reactions reached equilibrium. The data are compared with our model prediction (in which dispersion was set to zero) in Figure 8; species and reactions considered in the simulation are given in Tables 4 to 6. The predicted plateaus in pH and Al concentration are close to those observed (note that Al is very small), but the predicted plateau Si concentration exceeds the observed value by a factor of 4. Iler (1979) has noted that a damaged layer forms when strong NaOH contacts silica. This damaged layer can inhibit dissolution, preventing solution Si concentrations from reaching true equilibrium levels.

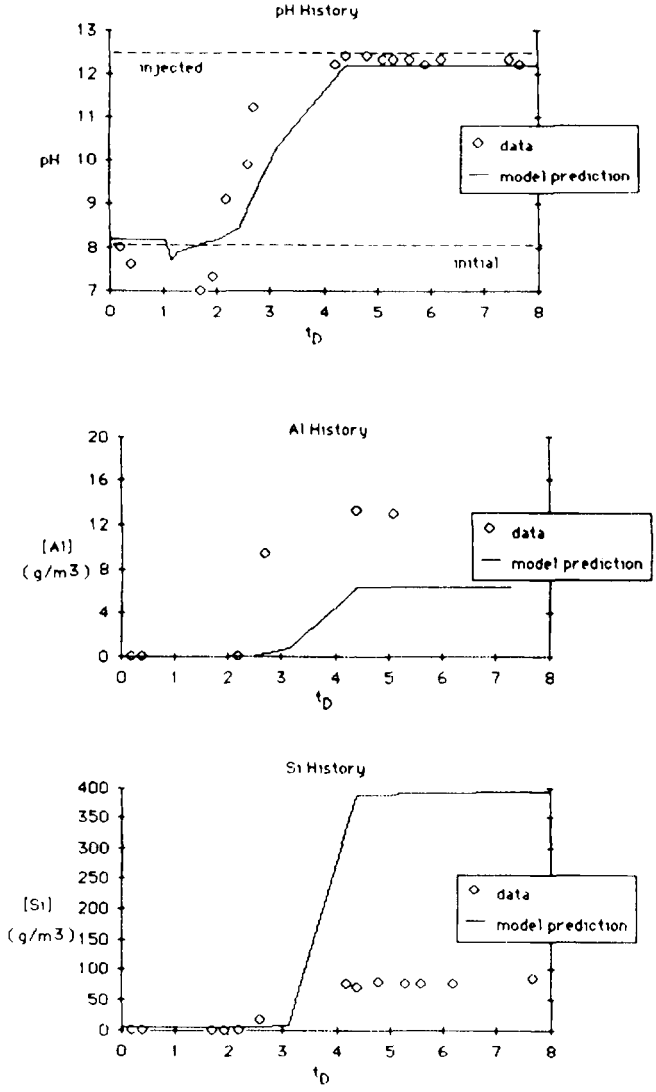

Figure 8. Model predictions for NaOH core flood (Bunge and Radke, 1982).

Bunge et al. (1980) injected high-pH brine into a calcium-saturated Wilmington sandstone and reported the calcium and pH histories shown in Figure 9. Model predictions for these floods are also shown in Figure 9. The experimentally observed hydroxide delay is smaller and pH loss larger than predicted, consistent with the conservative nature of our equilibrium-based estimates.

Bunge and Radke (1982) present pH histories for several alkaline floods in oil-bearing Wilmington sand. Four of these are shown in Figure 10. Using the same parameters as in the previous simulations, the model again accurately predicts pH breakthrough and pH loss for each flood but one. Again the pos-

Table 4. Species Considered in Alkaline Flooding Simulations

Solid Phase	Aqueous Phase	
$Al_2Si_2O_5(OH)_4$ (kaolinite)	OH^-	CO_3^-
SiO_2 (quartz)	H^+	HCO_3^-
$NaAlSi_2O_6H_2O$ (analcite)	H_4SiO_4	H_2CO_3
$KAl_3Si_3O_{10}(OH)_2$ (muscovite)	$H_3SiO_4^-$	Fe^{++}
$CaCO_3$ (calcite)	$H_2SiO_4^=$	$Fe(OH)^+$
CaH_2SiO_4	Al^{+++}	Na^+
$Ca(OH)_2$ (anhydrite)	$Al(OH)^{++}$	Ca^{++}
$FeCO_3$ (siderite)	$Al(OH)_2^+$	$Ca(OH)^+$
$Fe(OH)_2$	$Al(OH)_4^-$	K^+
$Al(OH)_3$		
Sorbed Species		
Ca^{++}		
Na^+		
H^+		

sibility of kinetic or mass transfer limitations makes the equilibrium prediction conservative.

Simplified evaluation of alkaline floods

The preceding examples show that the equilibrium model simulates the qualitative features of alkaline flooding and provides a conservative estimate of quantitative features. An idealized pH history for an alkaline flood, Figure 11, depicts these qualitative features. The elution of the hydroxide front is delayed by ion exchange. The plateau pH (useful pH) following

Table 5. Mineral Dissolution Reactions Considered in Alkaline Flooding Simulations

Solid Phase	Constituents	log K^{sp}
$Al_2Si_2O_5(OH)_4$	$= 2\,Al^{+3} + 2\,H_4SiO_4 + 6\,OH^- - 5\,H_2O$	−77.4
SiO_2	$= H_4SiO_4 - 2H_2O$	−4.0
$NaAlSi_2O_6H_2O$	$= Na^+ + Al^{+3} + 2\,H_4SiO_4 + 4\,OH^- - 5\,H_2O$	−46.0
$KAl_3Si_3O_{10}(OH)_2$	$= K^+ + 3Al^{+3} + 3\,H_4SiO_4 + 10\,OH^- - 10\,H_2O$	−109.6
$FeCO_3$	$= Fe^{+2} + CO_3^-$	−8.8
$Fe(OH)_2$	$= Fe^{+2} + 2\,OH^-$	−12.1
$CaCO_3$	$= Ca^{+2} + CO_3^-$	−8.1
$Ca(OH)_2$	$= Ca^{+2} + 2\,OH^-$	−4.3
CaH_2SiO_4	$= Ca^{+2} + H_2SiO_4^=$	−11.2
$Al(OH)_3$	$= Al^{+3} + 3\,OH^-$	−33.9

Table 6. Intraaqueous Reactions Considered in Alkaline Flooding Simulations

Aqueous Species	Constituents	log K
H^+	$= H_2O - OH^-$	14.0
$H_3SiO_4^-$	$= H_4SiO_4 + OH^- - H_2O$	−4.0
$H_2SiO_4^=$	$= H_4SiO_4 + 2\,OH^- - 2\,H_2O$	−5.0
$Al(OH)^{+2}$	$= Al^{+3} + OH^-$	−9.0
$Al(OH)_2^+$	$= Al^{+3} + 2\,OH^-$	−19.0
$Al(OH)_4^-$	$= Al^{+3} + 4\,OH^-$	−33.1
HCO_3^-	$= CO_3^- - OH^- + H_2O$	4.1
H_2CO_3	$= CO_3^- - 2\,OH^- + 2\,H_2O$	11.6
$FeOH^+$	$= Fe^+ + OH^-$	−4.5
$CaOH^+$	$= Ca^{+2} + OH^-$	−1.15

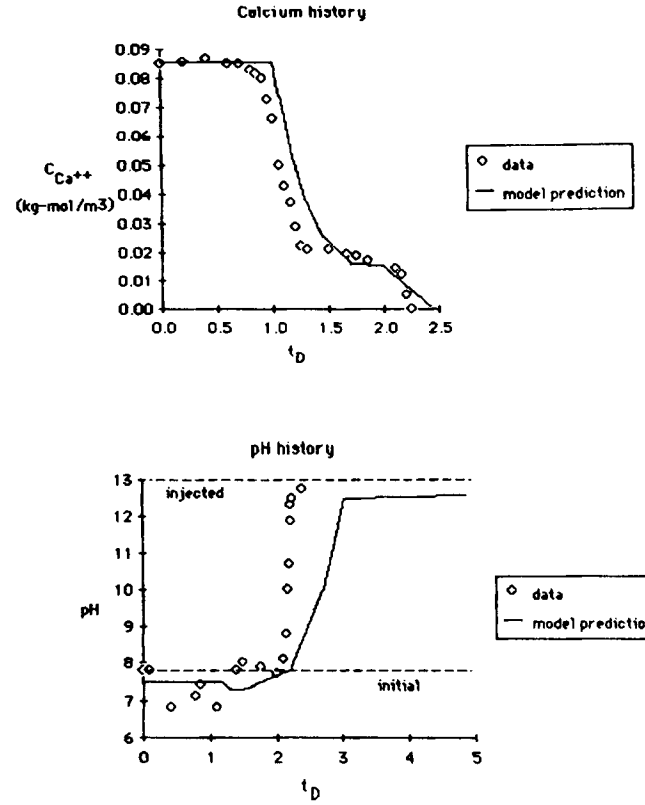

Figure 9. Model predictions for NaOH core flood (Bunge et al., 1980)

the hydroxide front is lower than the injected pH; this depletion is the pH loss. Given the adequacy of the equilibrium assumption, we can derive simple procedures for evaluating hydroxide breakthrough and pH loss that do not require running the model.

Model simulation and alkaline floods in sandstones suggests that the formation of $H_3SiO_4^-$(aq) and $H_2SiO_4^=$(aq) from dissolved silica accounts for most of the consumption of injected hydroxide. Thus we may estimate the pH loss by calculating the equilibrium state resulting from contacting the injected fluid with silica. To carry out this equilibration we write a charge balance, neglecting minor and nonreacting species:

$$[OH^-]_{inj} + [H_3SiO_4^-]_{inj} + 2[H_2SiO_4^=]_{inj} = [OH^-]_{eq} + [H_3SiO_4^-]_{eq} + 2[H_2SiO_4^=]_{eq} \quad (11)$$

The subscripts *inj* and *eq* in Eq. 11 refer to the injected compositions (given) and the equilibrated compositions (to be calculated).

The advantage of injecting buffered silicate solutions is apparent from this equation. If the injected silicate species concentrations are in equilibrium with silica at the injected pH, little silica dissolution will occur when the injected fluid contacts the rock, and pH loss is minimized. A laboratory flood of sodium orthosilicate (Bunge and Radke, 1982), demonstrates this effect, Figure 10b.

The dissociation of silica is given by

$$SiO_2 + 2H_2O = H_4SiO_4, \quad K_0 = [H_4SiO_4] \quad (12)$$

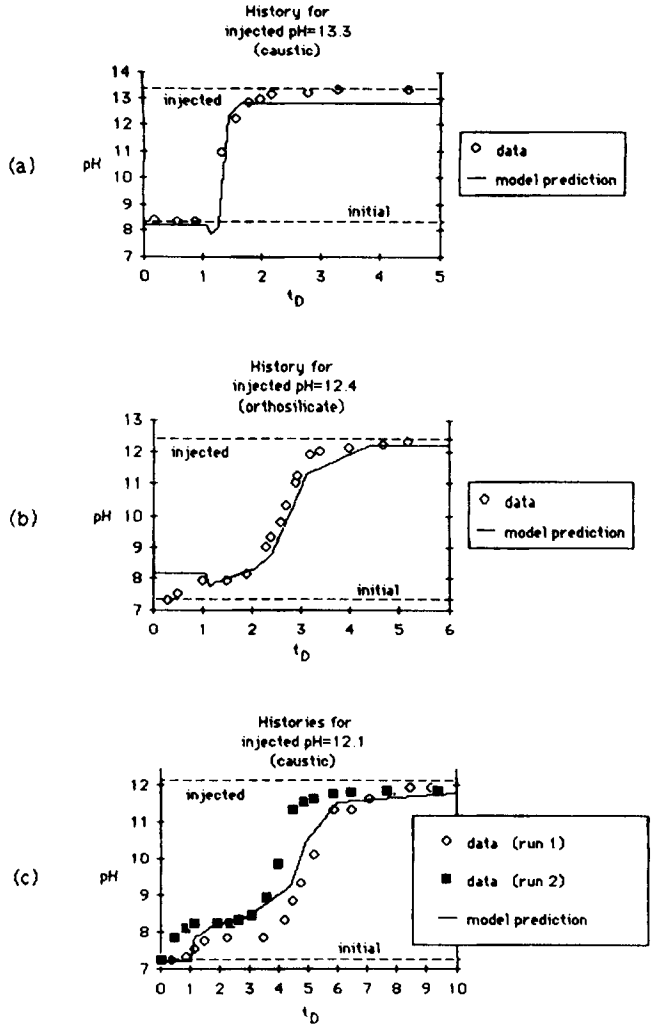

(a) (b) (c)

Figure 10. Model predictions for alkaline core floods (Bunge and Radke, 1982).

$$H_4SiO_4 + OH^- = H_3SiO_4^- + H_2O,$$

$$K_1 = [H_3SiO_4^-]/([OH^-][H_4SiO_4]) \quad (13)$$

$$H_4SiO_4 + 2OH^- = H_2SiO_4^{=} + 2H_2O,$$

$$K_2 = [H_2SiO_4^{=}]/([OH^-]^2[H_4SiO_4]) \quad (14)$$

Using the equilibrium expressions of Eqs. 12–14 in Eq. 11, we obtain

$$[OH^-]_{eq} = \{-(1 + K_0K_1) + [(1 + K_0K_1)^2 + 8K_0K_2[INJ]]^{1/2}\}/4K_0K_2 \quad (15)$$

where $[INJ]$ is the left side of Eq. 11. If kinetic limitations inhibit silica dissolution, hydroxide consumption will not reach the thermodynamically possible maximum, and calculated pH loss will be overestimated.

Calculated plateau pH values are shown in Table 7 for several floods reported in Bunge et al. (1980), Bunge and Radke (1982), and Sydansk (1982). Included in Table 7 are the plateaus observed in these experiments. Agreement is good for the lower pH floods, while the higher pH floods demonstrate the conservative nature of the theory.

The ion exchange characteristics of the medium are the chief factors determining the speed of the alkaline agent. If a single exchange reaction is important, this speed may be readily obtained from the sorption isotherm for that exchange. A sodium-hydrogen exchange isotherm is shown in Figure 12 (Bunge and Radke, 1982). Calculated breakthrough times based on this isotherm for several floods reported in Bunge and Radke (1982) and Sydansk (1982) are given in Table 7.

This estimate of hydroxide breakthrough time assumes that the injected fluid travels through the medium undepleted. Since the concentration of the fluid actually in contact with the rock determines the velocity of that concentration, taking depletion of the injected concentration into account should provide a better estimate of breakthrough time, Figure 12. Inasmuch as the calculated pH loss is conservative, the calculated breakthrough time will be conservative. Calculated breakthrough times accounting for pH losses calculated in Table 7 are also shown in the table.

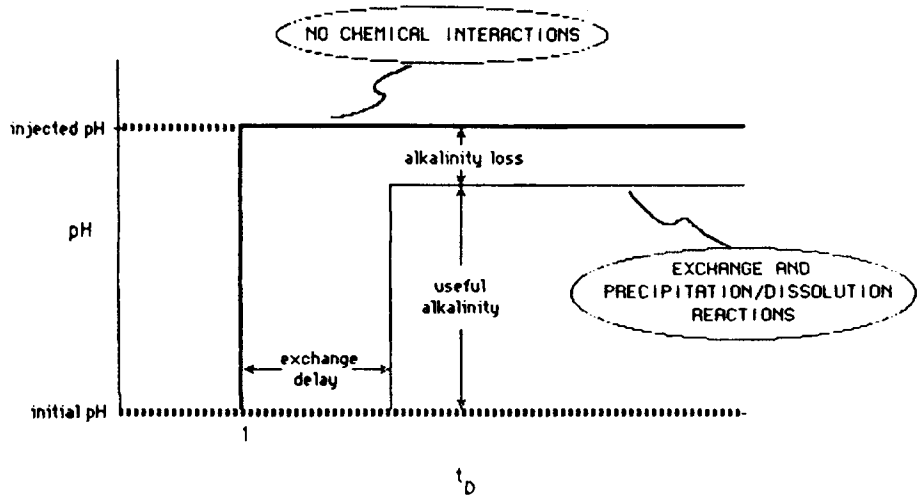

Figure 11. Idealized pH history for typical alkaline flood.

Table 7. Equilibrium Theory Estimate of Alkalinity Loss and Hydroxide Breakthrough Time for Several Laboratory Caustic Floods

Inj. pH	Useful Alkalinity (pH) Est. from Eq. 15	Obs.	Breakthrough Time (PV) Est.	Obs.	Est Using Calc. Alkalinity Loss	Reference
14.0	13.3	13.8	1.05	1.0	1.3	Sydansk (1982)
13.3	12.8	13.3	1.25	1.4	1.7	Bunge and Radke (1982)
13.2	12.7	13.1	1.32	1.1	1.8	Bunge and Radke (1982)
13.0	12.6	12.9	(Na/Ca/H exchange)*			Bunge et al. (1980)
12.5	12.1	12.2	2.19	2.6	3.2	Bunge and Radke (1982)
12.1	11.8	11.8	3.34	4.1	5.1	Bunge and Radke (1982)
12.1	11.8	11.8	3.34	5.2	5.1	Bunge and Radke (1982)

Equilibrium constants: $\log K_0 = -4.0$, $\log K_1 = 4.0$, $\log K_2 = 5.0$

*Simplified breakthrough calculation considers only sodium-hydrogen exchange.

Summary and Conclusions

We have successfully augmented our geochemical flow model (Walsh et al., 1984; Walsh, 1983) to include ion exchange of an arbitrary number of aqueous species on an arbitrary number of both insoluble and soluble exchangers. The model, which we believe to be the most general of its kind in existence, is based on local thermodynamic equilibrium.

We offer the following conclusions based on wave theory interpretation of model output:

1. Flows involving both precipitation/dissolution and ion exchange cannot be modeled by simple superposition of the two phenomena. Interaction between the two can result in wave behavior not possible with either alone.

2. The model successfully predicts the effluent from a number of experimental alkaline core floods. We modeled the permeable medium as silica with three clays that represented categories of the minerals normally present in the subject experiments. It was possible to match several diverse floods with only one set of parameters. In core floods where nonequilibrium effects were important the simulator confirmed that equilibrium calculations will give conservative estimates of pH loss.

3. We developed a simple procedure for estimating the useful pH and its rate of propagation. The procedure does not require running the model, but does provide reasonable, conservative estimates of hydroxide propagation rate and loss.

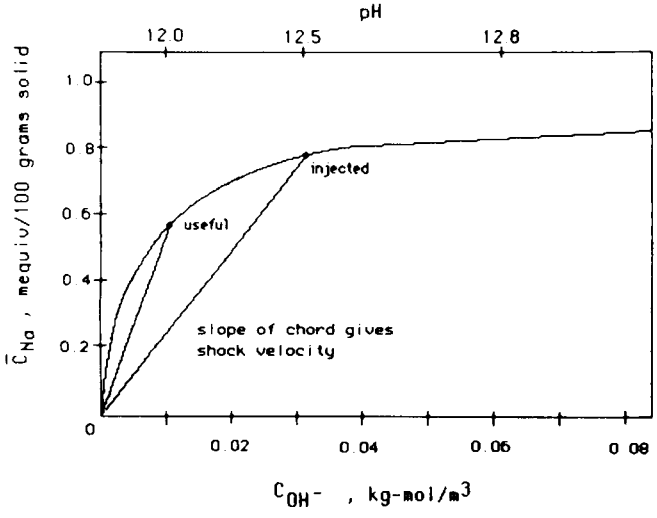

Figure 12. Sodium-hydrogen exchange isotherm (Bunge and Radke, 1982).

Acknowledgment

The research was supported by the Center for Enhanced Oil and Gas Recovery Research Program.

Notation

C_i^T = total concentration of element i, mol/L^3
C_j = concentration of fluid phase species j, mol/L^3
$\hat{C}_k$ = concentration of mineral k, mol/L^3
$\bar{C}_\ell$ = concentration of sorbed species ℓ, mol/L^3
$\bar{C}_v$ = concentration of vacant sites on a substrate, mol/L^3
$f_{i\ell}$ = stochiometric coefficient of element i in sorbed species ℓ
g_{ik} = stochiometric coefficient of element i in mineral k
h_{ij} = stochiometric coefficient of element i in fluid phase species j
I = number of elements in the system; number of independent fluid phase species in the system
J = number of fluid phase species in the system
K = number of mineral species possible in the system
K_p^{ex} = equilibrium constant for exchange reaction p
K_ℓ = dispersion coefficient
$K_{\ell j}$ = dispersion coefficient for fluid phase species j
K_r = equilibrium constant for formation of dependent fluid species r
K_k^{sp} = solubility product of mineral k
L = number of sorbed species possible in the system; characteristic length of system, L
M = number of substrates on which sorption can occur in the system
N_{Pe} = Peclet number; dimensionless inverse dispersion coefficient
P_r = concentration of dependent fluid phase species r in terms of the independent species
q_m = specific exchange/adsorption capacity of substrate m
Q_m = exchange/adsorption capacity of substrate m, mol/L^3
t = time, t
t_D = dimensionless time
u = bulk fluid phase superficial velocity, L/t
v = bulk fluid phase interstitial velocity (u/ϕ), L/t
v_{rj} = exponent of fluid species j in equilibrium expression for dependent species r
w_{kj} = exponent of fluid species j in solubility product expression for mineral k
x = distance, L
x_D = dimensionless position
$x_{p\ell}$ = exponent of sorbed species ℓ in exchange equilibrium expression p
y_{pj} = exponent of fluid phase species j in exchange equilibrium expression p
$z_{m\ell}$ = charge of sorbed species ℓ on substrate m
z_j = charge of flowing phase species j
Z = net charge of flowing phase
ϕ = porosity

Appendix

To outline one iteration of the equilibrium calculation procedure, suppose that K solids and M exchangers are present, Figure 1. The set of exchangers includes each of the K solids that have $q_m = 0$ and all the insoluble exchangers. Let L be the total number of bound species. The elemental totals and the surface charge balances provide $I + M$ equations in $J + K + L$ unknowns (C_j for $j = 1, \ldots, J$; $\hat{C}_k$ for $k = 1, \ldots, K$; $\bar{C}_\ell$ for $\ell = 1, \ldots, L$; recall that the C_i^T are known for this batch equilib-

rium calculation):

$$C_i^T = h_{ij}C_j + g_{ik}\hat{C}_k + f_{i\ell}\bar{C}_\ell \quad i = 1, \ldots, I$$
$$Q_m = z_{m\ell}\bar{C}_\ell \quad m = 1, \ldots, M \qquad \text{(A1)}$$

The charge balance on the ionic species in the fluid phase is simply a linear combination of the elemental totals. Thus any one of the I element balances in Eq. A1 may be replaced by the charge balance,

$$Z = z_j C_j \qquad \text{(A1a)}$$

where Z is the net charge of the fluid phase (usually zero). This substitution does not alter the mechanics of the subsequent procedure.

We algebraically eliminate the K solids concentrations from this set of equations (Walsh, 1983). Since solid concentrations may also appear in the surface charge balances (cf. Eq. 7), these balances must be included in the elimination process. Elimination yields $I + M - K$ equations in $J + L$ unknowns:

$$C_i^T = h'_{ij}C_j + f'_{i\ell}\bar{C}_\ell \quad i = 1, \ldots, I - n$$
$$Q_m = z'_{m\ell}\bar{C}_\ell \quad m = 1, \ldots, M - (K - n) \qquad \text{(A2)}$$

where n is the number of mass balances substituted for during the elimination. The primes indicate that constants from the elimination procedure are linear combinations of the stochiometric coefficients. If all K solids have zero exchange capacity, then no solid concentration appears in the surface charge balances, and $n = K$ and $z'_{m\ell} = z_{m\ell}$. To the set of Eq. (A2) we add the K solubility product constraints corresponding to the K solids, obtaining $I + M$ equations in $J + L$ unknowns:

$$C_i^T = h'_{ij}C_j + f'_{i\ell}\bar{C}_\ell \quad i = 1, \ldots, I - n$$
$$Q_m = z'_{m\ell}\bar{C}_\ell \quad m = 1, \ldots, M - (K - n)$$
$$K_k^{sp} = C_j^{w_{kj}} \quad k = 1, \ldots, K \qquad \text{(A3)}$$

We then substitute the equilibrium relations, Eq. 5, for the $J - I$ dependent fluid phase species concentrations in Eq. A3, yielding $I + M$ equations in $I + L$ unknowns:

$$C_i^T = h'_{ij}C_j + h'_{ir}P_r + f'_{i\ell}\bar{C}_\ell$$
$$Q_m = z'_{m\ell}\bar{C}_\ell$$
$$K_k^{sp} = (C_j^{w_{kj}})(P_r^{w_{kr}})$$
$$i = 1, \ldots, I - n$$
$$m = 1, \ldots, M - (K - n)$$
$$k = 1, \ldots, K \qquad \text{(A4)}$$

We perform a similar substitution in the $L - M$ exchange equilibria to obtain:

$$K_p^{ex} = (C_j^{y_{pj}})(P_r^{y_{pr}})(\bar{C}_\ell^{x_{p\ell}}) \quad p = 1, \ldots, L - M \qquad \text{(A5)}$$

Note that the summation and product on C_j in Eqs. A4 and A5 now range only over the I independent species.

We retain the sorbed concentrations as unknowns, despite their true mathematical status as dependent variables. Thus if we add the $L - M$ exchange equilibria, Eq. A5, to Eq. A4, we obtain $I + L$ equations in a like number of unknowns:

$$C_i^T = h'_{ij}C_j + h'_{ir}P_r + f'_{i\ell}\bar{C}_\ell$$
$$Q_m = z'_{m\ell}C_\ell$$
$$K_k^{sp} = (C_j^{w_{kj}})(P_r^{w_{kr}})$$
$$K_p^{ex} = (C_j^{y_{pj}})(P_r^{y_{pr}})(\bar{C}_\ell^{x_{p\ell}})$$
$$i = 1, \ldots, I - n$$
$$m = 1, \ldots, M - (K - n)$$
$$k = 1, \ldots, K$$
$$p = 1, \ldots, L - M \qquad \text{(A6)}$$

The concentrations of the I independent species and the L bound species that satisfy Eq. A6 are determined using a Newton-Raphson technique (recall that each P_r can be expressed in terms of the $C_j, j = 1, \ldots, I$). The $J - I$ dependent species concentrations, P_r, are then immediately calculated from Eq. 5, and the K solid concentrations are determined by difference from Eq. 2. This procedure constitutes one iteration of the equilibrium calculation.

Literature Cited

Boon, J. A., et al., "Reaction between Rock Matrix and Injected Fluids in Cold Lake Oil Sands—Potential for Formation Damage," *J. Canad. Pet. Tech.* (May–Aug., 1983).

Bryant, S. L., "Reactive Flow in Permeable Media," Ph.D. Diss., Univ. of Texas at Austin (1985).

Bunge, A. L., and C. J. Radke, "Migration of Alkaline Pulses in Reservoir Sands," *Soc. Pet. Eng. J.* (Dec., 1982).

Bunge, A. L., G. Klein, and C. J. Radke, "Divalent Ion Exchange with Alkali," SPE 8995, *5th Int. Symp. Oilfield and Geothermal Chem.*, Stanford, CA. (May, 1980).

Collins, R. E., *Flow of Fluids through Porous Materials*, Reinhold, New York, 139–200 (1961).

Cooke, C. E., Jr., R. D. Williams, and P. A. Kolodzie, "Oil Recovery by Alkaline Waterflooding," *J. Pet. Tech.* (Dec., 1974).

Crocker, M. E., E. C. Donaldson, and L. M. Marchin, "Comparison and Analysis of Reservoir Rocks and Related Clays," SPE 11973, *58th Ann. Tech. Conf. and Exhib.*, San Francisco (Oct., 1983).

De Zabala, E. F., et al., "A Chemical Theory for Linear Alkaline Flooding," *Soc. Pet. Eng. J.* (Apr., 1982).

Drever, James I., *The Geochemistry of Natural Waters*, Prentice Hall, New Jersey, 90–114 (1982).

Gao, H. W., H. Y. Sohn, and M. E. Wadsworth, "A Mathematical Model for the *in situ* Leaching of Primary Copper Ore," *Interfacing Technologies in Solution Mining*, W. J. Schlitt and J. B. Hiskey, eds., Proc. 2nd SME/SPE Int. Solution Mining Symp., Denver (Nov., 1981).

Garrels, R. M., and C. L. Christ, *Solutions, Minerals and Equilibria*, Harper and Row, New York, 352–370 (1965).

Helfferich, F., and G. Klein, *Multicomponent Chromatography*, Dekker, New York, 1–272 (1970).

Iler, Robert G., *The Chemistry of Silica*, Wiley, New York, 145–221 (1979).

Kabir, M. I., L. W. Lake, and R. S. Schechter, "A Minitest of *in situ* Uranium Leaching: Practical Problems in the Interpretation of Test Data," *In-Situ*, **6**(4), (1982).

Lake, L. W., and F. G. Helfferich, "Cation Exchange in Chemical Flooding. 2: The Effect of Dispersion, Cation Exchange, and Polymer/Surfactant Adsorption on Chemical Flood Environment," *Soc. Pet. Eng. J.* (Dec., 1978).

Lake, L. W., et al., "Isothermal, Multiphase, Multicomponent Fluid Flow in Permeable Media. I: Description and Mathematical Formulation," *In Situ*, **8**(1), (Mar., 1984).

Lax, P. D., "Hyperbolic Systems of Conservation Laws II," *Commun. Pure Appl. Math.* (Nov., 1957).
Levenspiel, O., *Chemical Reaction Engineering,* Wiley, New York, 426–475 (1962).
Lyklema, J., "Points of Zero Charge in the Presence of Specific Adsorption," *J. Coll. Interfac. Sci.* (May, 1984).
Miller, C. W. and L. V. Benson, "Simulation of Solute Transport in a Chemically Reactive Heterogeneous System: Model Development and Application," *Water Resources Res.* (Apr., 1983).
Mohnot, S. M., J. H. Bae, and W. L. Foley, "A Study of Mineral-Alkali Reactions," SPE 13032, *59th Ann. Tech. Conf. and Exhib.,* Houston (Sept., 1984).
Reed, M. G., "Gravel Pack and Formation Sandstone Dissolution During Steam Injection," *J. Pet. Tech.* (Jun., 1980).
Rhee, H.-K., R. Aris, and N. Amundson, "Theory of Multicomponent Chromatography," *Proc. Roy. Soc. London* (1968).
Shaughnessy, C. M., and K. R. Kunze, "Understanding Sandstone Acidizing Leads to Improved Field Practices," *J. Pet. Tech.,* (Jul., 1981).
Smith, William, and Ronald Missen, *Chemical Reaction Equilibrium Analysis: Theory and Algorithms,* Wiley, New York, 14–36 (1982).
Southwick, J. G., "Solubility of Silica in Alkaline Solutions: Implications for Alkaline Flooding," SPE 12771, *1984 California Reg. Meet.,* Long Beach (Apr., 1984).
Surdam, R. C., and R. A. Sheppard, "Zeolites in Saline, Alkaline Lake Deposits," in *Natural Zeolites,* L. B. Sand and F. A. Mumpton, eds., Pergamon, Elmsford, NY (1978).
Sydansk, Robert, "Elevated Temperature Caustic-Sandstone Interaction—Implications for Improving Oil Recovery," *Soc. Pet. Eng. J.* (Aug., 1982).
Tatom, T. A., R. S. Schechter, and L. W. Lake, "Factors Influencing the *in situ* Acid Leaching of Uranium Ores," *Interfacing Technologies in Solution Mining,* W. J. Schlitt and J. B. Hiskey, eds., Proc. 2nd SME/SPE Int. Solution Mining Symp., Denver (Nov., 1981).
Treybal, Robert E., *Mass-Transfer Operations,* McGraw-Hill, New York, 491–568 (1968).
Vermeulen, T., G. Klein, and N. K. Hiester, "Adsorption and Ion Exchange," in *Chemical Engineer's Handbook,* R. H. Perry and C. H. Chilton, eds., 5th ed., McGraw-Hill, New York (1973).
Vetter, O. J., and V. Kandarpa, "Prediction of $CaCO_3$ Scale Under Downhole Conditions," SPE 8991, *1980 Int. Symp. Oilfield and Geothermal Chem.,* SPE of AIME, Stanford, CA (May, 1980).
Walsh, M. P., "Geochemical Flow Modeling," Ph.D. Diss., Univ. of Texas at Austin, 1983.
Walsh, M. P., L. W. Lake, and R. S. Schechter, "A Description of Chemical Precipitation Mechanisms and their Role in Formation Damage during Stimulation by Hydrofluoric Acid," *J. Pet. Tech.* (Sept., 1982).
Walsh, M. P., et al., "Chemical Interactions of Aluminum-Citrate Solutions with Formation Minerals," SPE 11799, SPE Int. Symp. *Oilfield and Geothermal Chem.,* Denver (June, 1983).
———, "Precipitation and Dissolution of Solids Attending Flow through Porous Media," *AIChE J.,* **30**(2), 317 (1984).

Manuscript received Jan. 17, 1985, and revision received June 24, 1985.